

## *Azotobacter vinelandii* Ferredoxin I

A SEQUENCE AND STRUCTURE COMPARISON APPROACH TO ALTERATION OF [4Fe-4S]<sup>2+/+</sup> REDUCTION POTENTIAL\*

Received for publication, September 14, 2001, and in revised form, November 6, 2001  
Published, JBC Papers in Press, November 9, 2001, DOI 10.1074/jbc.M108916200

Kaisheng Chen<sup>‡§</sup>, Yean-Sung Jung<sup>‡</sup>, Christopher A. Bonagura<sup>‡¶</sup>, Gareth J. Tilley<sup>¶\*\*</sup>,  
G. Sridhar Prasad<sup>‡§§</sup>, Vandana Sridhar<sup>‡§§§</sup>, Fraser A. Armstrong<sup>¶</sup>, C. David Stout<sup>‡‡</sup>,  
and Barbara K. Burgess<sup>‡¶¶</sup>

From the <sup>‡</sup>Department of Molecular Biology and Biochemistry and Irvine Research Unit in Macromolecular Structure, University of California, Irvine, California 92697, the <sup>¶</sup>Department of Chemistry, Oxford University, Oxford OX1 3QR, United Kingdom, and the <sup>‡‡</sup>Department of Molecular Biology, The Scripps Research Institute, La Jolla, California 92037

The reduction potential ( $E^0$ ) of the [4Fe-4S]<sup>2+/+</sup> cluster of *Azotobacter vinelandii* ferredoxin I (AvFdi) and related ferredoxins is ~200 mV more negative than the corresponding clusters of *Peptostreptococcus asaccharolyticus* ferredoxin and related ferredoxins. Previous studies have shown that these differences in  $E^0$  do not result from the presence or absence of negatively charged surface residues or in differences in the types of hydrophobic residues found close to the [4Fe-4S]<sup>2+/+</sup> clusters. Recently, a third, quite distinct class of ferredoxins (represented by the structurally characterized *Chromatium vinosum* ferredoxin) was shown to have a [4Fe-4S]<sup>2+/+</sup> cluster with a very negative  $E^0$  similar to that of AvFdi. The observation that the sequences and structures surrounding the very negative  $E^0$  clusters in quite dissimilar proteins were almost identical inspired the construction of three additional mutations in the region of the [4Fe-4S]<sup>2+/+</sup> cluster of AvFdi. The three mutations, V19E, P47S, and L44S, that incorporated residues found in the higher  $E^0$  *P. asaccharolyticus* ferredoxin all led to increases in  $E^0$  for a total of 130 mV with a 94-mV increase in the case of L44S. The results are interpreted in terms of x-ray structures of the Fdi variants and show that the major determinant for the large increase in L44S is the introduction of an OH-S bond between the introduced Ser side chain and the S $\gamma$  atom of Cys ligand 42 and an accompanying movement of water.

essential electron transfer reactions, including membrane-bound electron transport systems; their functions, however, are not restricted to electron transfer and include direct catalysis of hydration/dehydration reactions, O<sub>2</sub> and iron sensing, regulation of gene expression, iron storage, metal cluster assembly, and the generation and stabilization of radical intermediates (for reviews, see Refs. 1–6). To meet these diverse functions, individual proteins have increased the variety of [Fe-S] cluster structures by adding or subtracting iron and sulfide atoms to vary the cluster type, or by introducing noncysteine ligands. Even after adopting a specific cluster type (e.g. [4Fe-4S] clusters with four cysteine ligands), proteins can control reactivity further by stabilizing a particular redox couple (e.g. 3+/2+, 2+/+, or +/0) or by modulation of the reduction potential ( $E^0$ ) of a particular redox couple (7–19). Thus, high potential iron proteins have [4Fe-4S]<sup>3+/2+</sup>  $E^0$  ranging from 90 to 450 mV (7–16, 20), while ferredoxins that contain structurally indistinguishable [4Fe-4S]<sup>2+/+</sup> clusters have  $E^0$  ranging from –280 to –715 mV in different native proteins (10, 21).

Both experimental and theoretical research has been directed toward understanding how the polypeptide surrounding the cluster controls the reduction potential. Factors that have been proposed as being important include (a) solvent exposure of the cluster, (b) specific hydrogen bonding networks especially NH-S bonds, (c) the proximity and orientation of protein backbone and side chain dipoles, and/or (d) the proximity of charged residues to the cluster (7, 21–35). This study concerns protein control of the reduction potential of a [4Fe-4S]<sup>2+/+</sup> cluster that is ligated via a typical CXXCXXC motif with one remote Cys ligand.

Previous studies in this area have focused on comparing the environments of the clusters in structurally characterized proteins. The [4Fe-4S]<sup>2+/+</sup> cluster of *Azotobacter vinelandii* ferredoxin I (AvFdi)<sup>1</sup> has a low  $E^0$  of about –620 mV (pH 7.0) (36), whereas the analogous clusters in *Peptostreptococcus asaccharolyticus* ferredoxin (PaFd) and *Clostridium acididurici* ferredoxin have  $E^0$  of about –430 mV (not pH-dependent) (37). Comparison of the structures of these proteins showed that the peptide folding around the analogous clusters is highly conserved with respect to the location of the four Cys ligands, the Cys dihedral angles, and the eight amide groups hydrogen-

Most iron-sulfur ([Fe-S]) proteins are intimately involved in

\* This work was supported by National Institutes of Health Grants GM-45209 (to B. K. B.) and GM-48495 (to C. D. S.) and by a grant from UK EPSRC and BBSRC Grant 43/B11675 (to F. A. A.). The costs of publication of this article were defrayed in part by the payment of page charges. This article must therefore be hereby marked “advertisement” in accordance with 18 U.S.C. Section 1734 solely to indicate this fact.

The atomic coordinates and structure factors (code 1G3O, 1GAO, and 1G6B) have been deposited in the Protein Data Bank, Research Collaboratory for Structural Bioinformatics, Rutgers University, New Brunswick, NJ (<http://www.rcsb.org/>).

§ Present address: The Genomics Institute of the Novartis Research Foundation, 3115 Merryfield Row, Suite 200, San Diego, CA 92121.

¶ Present address: Plexxikon, Inc., 91 Bolivar Dr., Berkeley, CA 94710.

\*\* Present address: 31B Foxenden Rd., Guildford, Surrey GU2 4DL, United Kingdom.

§§ Present address: Emerald BioStructures Inc., Bainbridge Island, WA 98110.

¶¶ To whom correspondence should be addressed: Dept. of Molecular Biology and Biochemistry, University of California, Irvine, CA 92697. Tel.: 949-824-4297; Fax: 949-824-8551; E-mail: bburgess@uci.edu.

<sup>1</sup> The abbreviations used are: AvFdi and AvFdiIII, *A. vinelandii* ferredoxin I and III, respectively; PaFd, *P. asaccharolyticus* ferredoxin; CvFd, *C. vinosum* ferredoxin; Fd, ferredoxin; Fdi, ferredoxin I; MES, 4-morpholineethanesulfonic acid; EPR, electron paramagnetic resonance; TAPS, *N*-tris[hydroxymethyl]methyl-3-aminopropanesulfonic acid.

bonded to sulfur atoms of the cluster (22). Although early theoretical studies suggested that the solvent access to the [4Fe-4S]<sup>2+/+</sup> cluster of PaFd might explain its more positive  $E^0$  value, a more recent 0.95-Å structure of *C. acidiurici* ferredoxin failed to reveal the presence of internal water molecules (38). The proposal that negatively charged surface residues or hydrophobic residues near the [4Fe-4S]<sup>2+/+</sup> cluster of AvFdI might explain its more negative reduction potential (7, 23–28) was directly tested by converting six individual amino acid residues in AvFdI into the corresponding residue in PaFd (29). Those substitutions, however, failed to raise the  $E^0$  of the [4Fe-4S]<sup>2+/+</sup> cluster of AvFdI. Thus, at present both experimental and theoretical approaches have failed to determine what factors are responsible for the 200-mV difference in  $E^0$  for the [4Fe-4S]<sup>2+/+</sup> clusters of AvFdI versus PaFd and *C. acidiurici* ferredoxin.

In this study, we have extended the sequence/structure comparison approach to include a third class of ferredoxins and have achieved substantial increases in the  $E^0$  of the [4Fe-4S]<sup>2+/+</sup> cluster of AvFdI by substitution of individual residues.

#### EXPERIMENTAL PROCEDURES

**Mutagenesis of fdxA, Expression, Purification, and Crystallization of FdI Variants**—Site-directed mutagenesis was carried out as described elsewhere (29) using the following oligonucleotides: 5'-ACCGATTGTGTTGAAGAGTGCCCGGTAGACTGT-3' for V19E; 5'-GACTGCGCGAGCTGCGAGCCCGAGTGC-3' for L44S; and 5'-GCTCTGCGAGTCCGAGTGC-3' for P47S. Cell growth and the purification and triclinic crystallization of FdI variants were carried out as described elsewhere (39). All mutants accumulated to native levels in the cells.

**Protein Characterization**—EPR spectra were obtained using a Bruker ESP300E spectrometer, interfaced with an Oxford liquid helium cryostat. For spin quantitation of reduced [4Fe-4S]<sup>+</sup>, the spectrum of L44S after reduction by 4 mM sodium dithionite was recorded at 15 K using 60 μM purified L44S FdI at a microwave power<sup>1/2</sup> of 1 milliwatt. Under those conditions, the EPR signal of FdI is linearly proportional to (microwave power)<sup>1/2</sup>. A sample of 50 μM Cu<sup>2+</sup>-EDTA used as a standard was recorded at the same EPR setting and temperature, where the signal is also linearly increasing in the function of (power)<sup>1/2</sup>. Absorption spectra were recorded in 0.5-ml quartz cuvettes on a Hewlett Packard 8452A diode array spectrophotometer. CD spectra were obtained using a Jasco J-500C spectropolarimeter. For UV-visible and CD measurements of reduced sample, 4 mM sodium dithionite was added to samples in a Vacuum Atmospheres anaerobic chamber. UV-visible and CD measurements were carried out using 1-ml volume cylindrical cells with fused quartz windows.

**Electrochemistry**—Purified water of resistivity ~18 megaohms-cm (Millipore) was used in all experiments. The buffers MES, HEPES, and TAPS and the co-adsorbate neomycin sulfate were purchased from Sigma. An AutoLab electrochemical analyzer (EcoChemie, Utrecht, The Netherlands) was used to record DC voltammograms. The three-electrode configuration featuring all glass cells has been described previously (40). The sample compartment (typically holding 500 μl) was maintained at 0 °C to optimize stability. All  $E^0$  values are given with reference to the standard hydrogen electrode. The saturated calomel electrode was held at 22 °C, which we have adopted as  $E$  (saturated calomel reference electrode) = +243 mV versus standard hydrogen electrode (41).  $E^0$  values from cyclic voltammetry were calculated as the average of the anodic and the cathodic peak potentials,  $E^0 = 1/2(E_{pa} + E_{pc})$ . The pyrolytic graphite "edge" electrode (surface area typically 0.18 cm<sup>2</sup>) was polished prior to each experiment with an aqueous alumina slurry (Buehler Micropolish; 1.0 μm) and then sonicated extensively to remove traces of Al<sub>2</sub>O<sub>3</sub>. All experiments were carried out under anaerobic conditions in a glove box (Vacuum Atmospheres Company) with an inert atmosphere of N<sub>2</sub> (O<sub>2</sub> < 1.0 ppm).

Prior to electrochemical experiments, all protein samples were checked for purity by running fast protein liquid chromatography (Amersham Biosciences, Inc., Uppsala, Sweden) with a Mono Q column equilibrated with 0.05 M Tris, pH 7.4, and a linear gradient from 0.05 to 1 M NaCl. Bulk electrochemistry solutions contained 0.05–0.1 mM protein in 60 mM mixed buffer (15 mM Tris, 15 mM MES, 15 mM TAPS, 15 mM acetate), with 0.1 M NaCl as supporting electrolyte and 4 mM neomycin. Neomycin stabilizes the protein-electrode interactions. For

$E^0$	Fd	cluster						
-620 mV	AvFdI	2	35	HPDECIDCALCEP	47	19	VCFVDF	25
-650 mV	CvFd	1	4	ITDECINCVCEP	16	52	VCFVDCI	58
-650 mV	AvFdIII	1	4	ITDDCINCVCEP	16	52	VCFVDCI	58
-430 mV	PaFd	2	32	DADSCIDCGSCAS	44	17	ECFVNCI	23

FIG. 1. Comparison of the sequences near the low potential [4Fe-4S]<sup>2+/+</sup> clusters of three structurally characterized ferredoxins: AvFdI (Protein Data Bank code 7FD1), PaFd (Protein Data Bank code 1DUR), CvFd (Protein Data Bank code 1BLU), and AvFdIII. Amino acids in blue represent mutations previously characterized (29). The amino acids in red represent the residues of interest in this study. Cluster numbers refer to the position of the cluster relative to the NH<sub>2</sub> terminus of the protein.

the investigation of pH dependence, protein solutions were dialyzed extensively against the buffered solution at the required pH, using an Amicon 8MC diafiltration unit equipped with a microvolume assembly and a YM-3 membrane, or by the addition of 15 μl of stock protein solution in 50 mM Tris, 0.1 M NaCl, pH 8.0, to 385 μl of the required buffer. The pH of the solution was checked after each experiment.

**Structure Determination**—Tetragonal crystals of the V19E and P47S FdI mutants were grown as previously described (32). Data for the V19E and P47S mutants were collected using an R-AXIS IV imaging plate, Osmic mirrors, and a Rigaku RU300 rotating anode x-ray source equipped with an Crystal Logic N<sub>2</sub> cryogenic system; data for the L44S mutant were collected at Stanford Synchrotron Radiation Laboratory beam line 7-1. The structures were solved by molecular replacement. The V19E FdI structure was refined to 1.65-Å resolution with  $R = 0.249$  and  $R_{free} = 0.265$ ; the P47S FdI structure was refined to 1.90-Å resolution with  $R = 0.240$  and  $R_{free} = 0.266$ . Monoclinic crystals of L44S FdI were grown as for native FdI with the addition of 200 mM lithium sulfate to the reservoir solution. The space group is C2 with  $a = 130.8$ ,  $b = 85.6$ ,  $c = 67.2$  Å,  $\beta = 117.9^\circ$ , and four molecules in the asymmetric unit. The structure was solved by molecular replacement and refined to 2.20-Å resolution with  $R = 0.243$  and  $R_{free} = 0.286$ . Details of the data collection and refinement for each mutant FdI structure determination are included in the Protein Data Bank depositions. The coordinates for the structures of the V19E, L44S (four independent structures), and P47S mutants of FdI have been deposited in the Protein Data Bank with accession codes 1G30, 1GAO, and 1G6B, respectively.

#### RESULTS AND DISCUSSION

**Selection of Mutants**—Eight-iron ferredoxins containing two [4Fe-4S]<sup>2+/+</sup> clusters have long been known to fall into two general classes with respect to sequence motifs. The "clostridial-type" ferredoxins, represented by the structurally characterized PaFd and *C. acidiurici* ferredoxin, are  $M_r \sim 5,550$  proteins where both clusters receive three of their four ligands from a CXXCXXC motif (1–6, 22, 38, 42, 43). The other class is represented by the structurally characterized,  $M_r$  9,058 *Chromatium vinosum* ferredoxin (CvFd), which has one cluster ligated by a CXXCXXC motif and the other ligated by a CXXCX<sub>8</sub>C motif (42, 44). Regardless of these differences in sequence motif, both classes of proteins have long been believed to contain two [4Fe-4S]<sup>2+/+</sup> clusters of equivalent  $E^0$  (10, 42). This view was challenged in 1998 by our discovery that a ferredoxin from *A. vinelandii* (AvFdIII) was very similar to CvFd based on molecular weight and sequence motif and yet had very different  $E^0$  values of -486 and -644 mV for its two [4Fe-4S]<sup>2+/+</sup> clusters (45). A reexamination of CvFd then led to the conclusion that it also had very different  $E^0$  of about -460 mV and about -655 mV for its two [4Fe-4S]<sup>2+/+</sup> clusters (46, 47). These studies further identified the lower  $E^0$  cluster of CvFd as the one with the CXXCXXC motif.

The similarity of  $E^0$  values for the [4Fe-4S]<sup>2+/+</sup> cluster of AvFdI (-620 mV at pH 7.0) and the lower  $E^0$  clusters of AvFdIII and CvFd led us to extend the sequence and structure comparison to include these proteins. Fig. 1 compares the sequences around the [Fe-S] clusters of PaFd, AvFdI, CvFd, and AvFdIII. Although clearly evolutionarily related (48), PaFd and AvFd vary greatly in size ( $M_r$  5,556 versus 12,050) and cluster composition (8Fe versus 7Fe), and they share only 48% sequence similarity in their first 50 amino acids, where the clus-

ters are located. As in previous studies (10, 22, 29), the homologous [4Fe-4S]<sup>2+/+</sup> clusters (*i.e.* the second cluster from the NH<sub>2</sub> terminus) are being compared, with *PaFd* having an  $E^{0'}$  value ~200 mV more positive than the corresponding cluster in *AvFdI*. *AvFdI* and *CvFd* also vary greatly in size ( $M_r$ , 12,050 versus 9,058) and cluster composition (7Fe versus 8Fe) and share only 42% sequence similarity in their first 50 amino acids, where the clusters are located. In this case, however, it is the first cluster from the NH<sub>2</sub> terminus of *CvFd* that has a very low  $E^{0'}$  value, similar to the second cluster from the NH<sub>2</sub> terminus of *AvFdI*. Despite these differences, Fig. 1 shows that the sequences surrounding the two low  $E^{0'}$  clusters in *AvFdI* and *CvFd* (or *AvFdIII*) are extremely similar to each other.

In a previous study, we constructed D23N, F25I, H35D, E38S, and E46A variants of *AvFdI* (Fig. 1) and found no change in  $E^{0'}$  (29). Based on the sequence comparisons shown in Fig. 1 and based on the protein structures, we have now constructed and characterized V19E, L44S, and P47S variants of *AvFdI* in attempts to mimic their positions in *PaFd* for which  $E^{0'}$  is higher. The residues corresponding to Val<sup>19</sup> and Pro<sup>47</sup> are completely conserved in the low  $E^{0'}$  classes of ferredoxins. As discussed elsewhere, the residue corresponding to Leu<sup>44</sup> varies, and in the low  $E^{0'}$  ferredoxins, it is generally Leu or Val or occasionally Met (46). The selection of these mutations was further encouraged by theoretical and experimental studies showing positive changes in  $E^{0'}$  induced by substitution of nonpolar residues (*e.g.* Leu and Val) by polar residues, including serine (32, 49). Fig. 2A is an overlay of the homologous [4Fe-4S]<sup>2+/+</sup> clusters of *CvFd* and *AvFdI*, showing their similarity in this region. Fig. 2B is an overlay of the same region of *AvFdI* and *PaFd*, showing the positions in the native proteins of the three residues under consideration relative to the cluster.

**Purification and Characterization of the FdI Variants**—The V19E, L44S, and P47S variants of *AvFdI* were constructed, expressed in their native background in *A. vinelandii*, and purified as described under “Experimental Procedures.” These variants were all air-stable and accumulated to levels similar to that of native FdI in the cell. Fig. 3 compares the UV-visible absorption spectra of each of the variants with those of native FdI, both in their air-oxidized states and following the anaerobic addition of dithionite. The oxidation states of the clusters in the presence of air are [4Fe-4S]<sup>2+</sup> and [3Fe-4S]<sup>+</sup>. For native FdI, dithionite reduces only the [3Fe-4S]<sup>+</sup> cluster to the “zero” oxidation level but does not reduce the [4Fe-4S]<sup>2+</sup> cluster because its reduction potential is too low (36, 50). This result is also obtained for V19E and P47S variants. In contrast, as shown in Fig. 3, dithionite causes considerably more reversible bleaching of L44S, suggesting that the  $E^{0'}$  value for its [4Fe-4S]<sup>2+/+</sup> cluster has increased relative to native FdI. This reduction of the [4Fe-4S]<sup>2+</sup> cluster in L44S was confirmed by EPR spectroscopy.

As shown in Fig. 4, air-oxidized FdI exhibits a characteristic  $g = 2.01$  EPR signal that arises from the [3Fe-4S]<sup>+</sup> cluster having  $S = 1/2$ . Val<sup>19</sup>, Leu<sup>44</sup>, and Pro<sup>47</sup> are all remote from that cluster, and, as expected, the mutation of these residues did not influence that signal. Consistent with the data shown in Fig. 3, the anaerobic addition of dithionite to V19E and P47S FdIs led to reduction of the [3Fe-4S]<sup>+</sup> cluster to the “zero” oxidation level and disappearance of the  $g = 2.01$  signal but did not result in reduction of the [4Fe-4S]<sup>2+</sup> cluster, the same result that is obtained for native FdI (36). For L44S, the [4Fe-4S]<sup>2+</sup> cluster could be partially reduced by dithionite (Fig. 4), thereby confirming the conclusion from the UV-visible absorption experiment (Fig. 3). Spin quantitation of the signal of the [4Fe-4S]<sup>+</sup> cluster using Cu-EDTA showed that 20% of the L44S [4Fe-4S]<sup>2+</sup> cluster was reduced by dithionite, consistent with the  $E^{0'}$

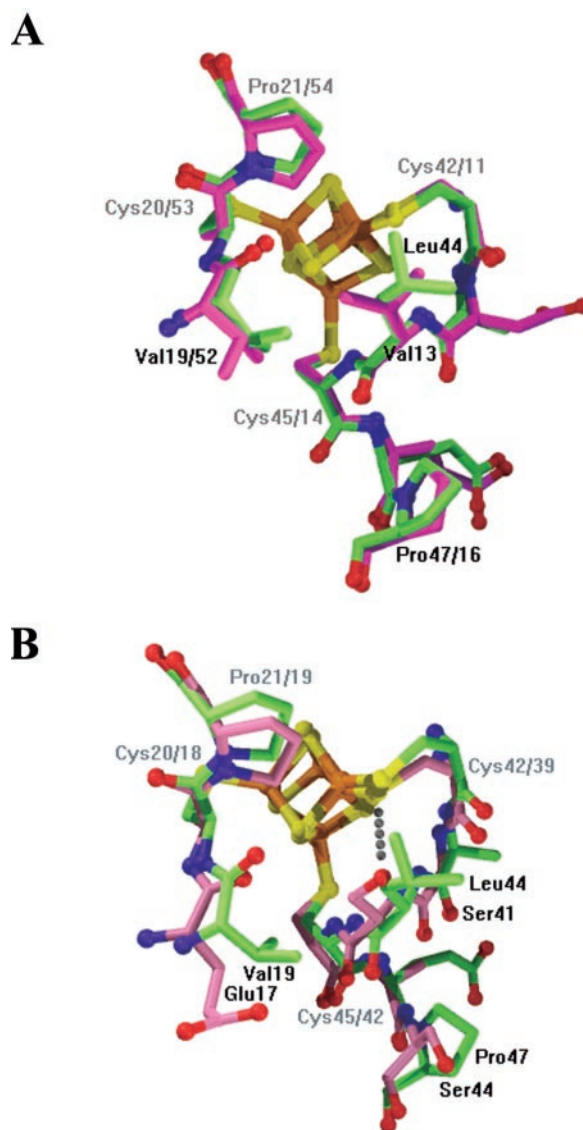


**FIG. 2. Superposition of the [4Fe-4S] cluster binding regions in three ferredoxins with differing reduction potentials.** In A and B, *AvFdI* residues mutated in this study and the corresponding residues in *CvFd* and *PaFd* are highlighted with *black labels*. A, superposition of residues 19–21 and 42–47 of *AvFdI* (green) with residues 52–54 and 11–16, respectively, of *CvFd* (purple) (Protein Data Bank accession code 1BLU) and the corresponding [4Fe-4S] clusters coordinated by each protein. The superposition is based on least squares fit of residues 19–25 and 38–47 of *AvFdI* with residues 52–58 and 7–16 of *CvFd* (root mean square deviation 0.33 Å for 17 Cα atoms). B, superposition of residues 19–21 and 42–47 of *AvFdI* (green) with residues 17–19 and 39–44, respectively, of *PaFd* (pink) (PDB accession code 1DUR) and the corresponding [4Fe-4S] clusters coordinated by each protein. The superposition is based on least squares fit of 54 homologous Cα atoms in the two proteins identified by a structure based sequence alignment (root mean square deviation 0.88 Å). A hydrogen bond in *PaFd* involving Ser<sup>41</sup> and Cys<sup>39</sup> is shown as a gray dotted line (3.45 Å).

data discussed below. The wavelength dependence and form of the CD spectra of oxidized and reduced native FdI and V19E, L44S, and P47S variants are extremely similar (Fig. 5). In previous studies of variants that showed structural rearrangements in the vicinity of the [4Fe-4S]<sup>2+/+</sup>, the CD spectra were dramatically different (36, 49, 51). Thus, the CD data, combined with the UV-visible and EPR strongly suggest that the overall protein folding in solution and the environment around the clusters has not been significantly perturbed in any of the altered proteins.

**Reduction Potential Measurements**—The  $E^{0'}$  values for the

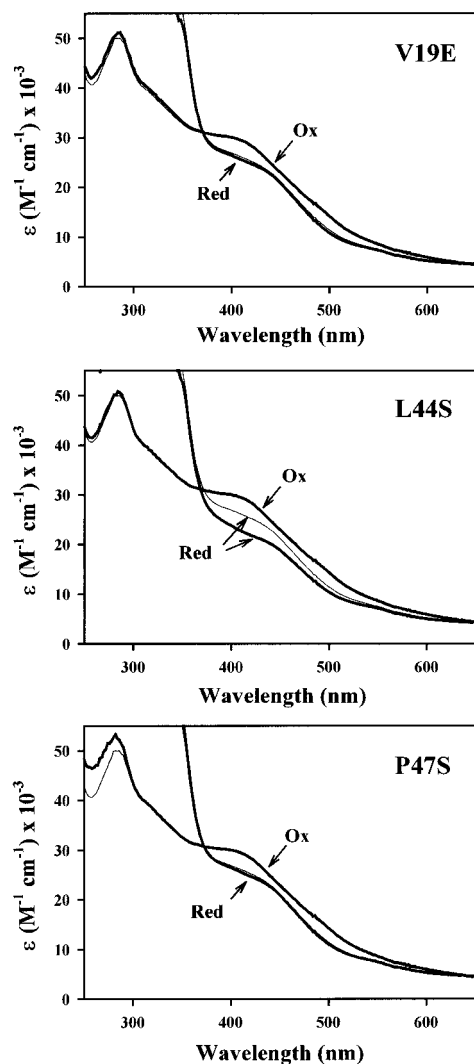


FIG. 3. UV-visible absorption spectra of native FdI (thin lines) compared with the V19E, L44S, and P47S FdI variants (thick lines). Ox, spectra for oxidized FdI; Red, spectra for reduced FdI. The protein samples were contained in 50 mM Tris-HCl, pH 7.4. The reduced proteins were prepared by the addition of 2 mM in  $\text{Na}_2\text{S}_2\text{O}_4$  to degassed samples.

[Fe-S] clusters of native FdI, V19E, L44S, and P47S were measured under identical conditions using voltammetric methods as described under "Experimental Procedures." Results obtained at pH 7.0, for ferredoxin solutions containing 4 mM neomycin, are shown in Fig. 6. Two pairs of well defined oxidation and reduction peaks are observed in each case, with the higher  $E^{0'}$  peaks corresponding to oxidation/reduction of the  $[3\text{Fe-4S}]^{+/0}$  cluster and the lower  $E^{0'}$  peaks corresponding to oxidation/reduction of the  $[4\text{Fe-4S}]^{2+/+}$  cluster (40). The mutations were all remote from the  $[3\text{Fe-4S}]^{+/0}$  cluster, and, as expected from previous studies (e.g. see Refs. 29 and 36), no changes were observed in  $E^{0'}$  for that couple. The  $[4\text{Fe-4S}]^{2+/+}$  cluster  $E^{0'}$  of native FdI is known to be weakly pH-dependent, and the same pH dependence was observed for all of the variants examined in this study. Table I summarizes the data collected at pH 7.0 and shows that in all three cases positive changes in  $E^{0'}$  were observed. For V19E, the increase was 13 mV; for L44S, the increase was 94 mV; and for P47S, the increase was 23 mV. The electrochemical measurements for these mutants have an error of about  $\pm 10$  mV.

*X-ray Structures of the Variants*—X-ray structures of all three variants were obtained in order to determine whether the intro-

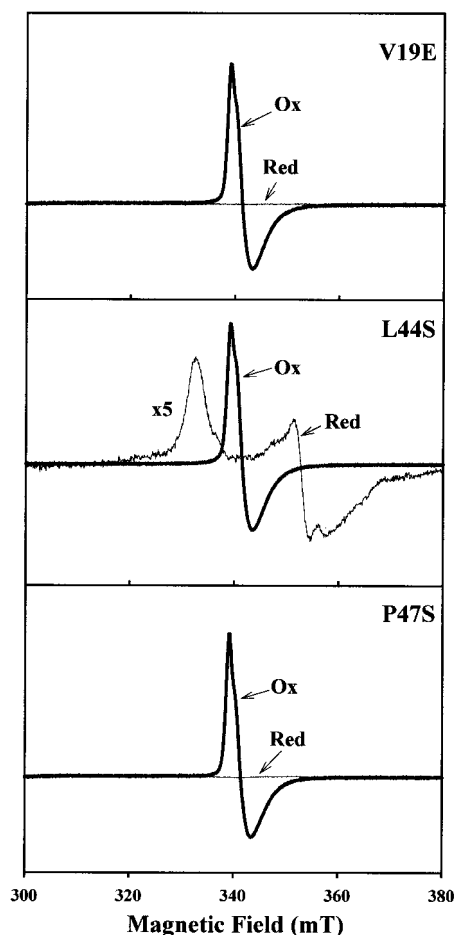


FIG. 4. EPR spectra of V19E, L44S, and P47S FdI variants in the oxidized (thick line; Ox) and reduced states (thin lines; Red). The reduced proteins were prepared by the addition of 4 mM in  $\text{Na}_2\text{S}_2\text{O}_4$  to degassed samples.

duced residues in AvFdI adopted the same orientations as in native PaFd and thus help interpret the observed changes in  $E^{0'}$ .

*V19E*—Fig. 7A compares the structure of V19E, refined to 1.65 Å, with that of native FdI in the region of the  $[4\text{Fe-4S}]^{2+/+}$  cluster, and Fig. 7B compares the orientation of Glu<sup>19</sup> in V19E with that of the corresponding residue in PaFd. Overall, the structure of V19E is very similar to that of native FdI, and there is virtually no difference between the native FdI and V19E structures at the position of Cys ligand 20. There is also no change in solvent accessibility as evidenced by no change in the packing around the  $[4\text{Fe-4S}]^{2+/+}$  cluster. When compared with PaFd, the introduced Glu is not exactly in the same orientation (Fig. 7B), but in both cases the distances to the cluster are very long, with the shortest distance from the Glu<sup>19</sup> Oε1 to the nearest sulfur atom of the  $[4\text{Fe-4S}]^{2+/+}$  cluster being 7.8 Å for V19E versus 8.6 Å for PaFd. Consistent with the similarities of the native FdI and V19E structures, V19E gave a barely perceptible positive increase in  $E^{0'}$  relative to native FdI. The fact that introducing a negatively charged surface residue, with a carboxylate to cluster distance of 7.8 Å, does not result in a significant change in  $E^{0'}$  is fully consistent with the initial study on surface charged residues (29).

*P47S*—Fig. 8A compares the structure of P47S, refined to 1.9 Å, with that of native FdI in the region of the  $[4\text{Fe-4S}]^{2+/+}$  cluster, whereas Fig. 8B compares the orientation of Ser<sup>47</sup> in P47S to that of the corresponding residue in PaFd. The side chain of Ser<sup>47</sup> came up clearly in the unbiased density, so there are no changes in the main chain, and, except at position 47,

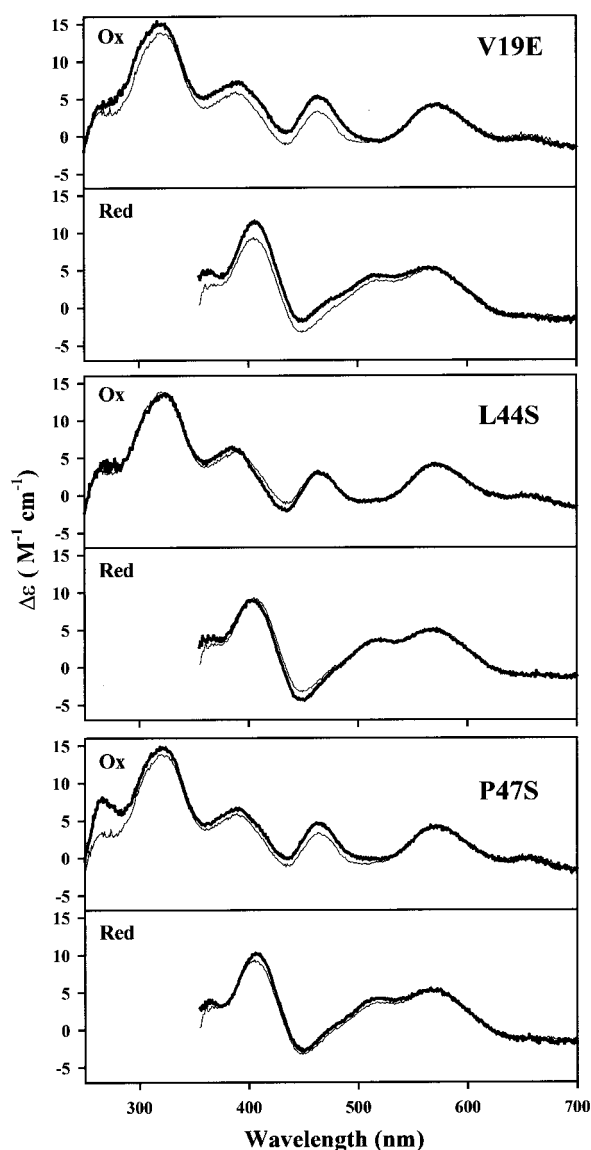


FIG. 5. CD spectra of native FdI (*thin lines*) and V19E, L44S, and P47S FdI variants (*thick lines*) in the oxidized and reduced states. *Ox*, spectra for oxidized FdI; *Red*, spectra for reduced FdI. The reduced proteins were prepared by the addition of 2 mM in  $\text{Na}_2\text{S}_2\text{O}_4$  to degassed samples.

the structure is indistinguishable from that of native FdI. In this case, a small 23-mV increase in  $E^{0'}$  was obtained, possibly due to the introduction of an OH dipole that is directed toward the cluster, albeit at a long distance. Three new ordered water molecules are also observed in P47S *versus* native FdI between the Ser<sup>47</sup> side chain and the carbonyls of Ala<sup>43</sup> and Leu<sup>44</sup>, but these do not increase solvent accessibility, since the packing around the cluster remains the same. (Note that these are also much farther from the  $[\text{4Fe-4S}]^{2+/1+}$  cluster, at 8–10 Å, *versus* the new waters in L44S, which had a much greater increase in  $E^{0'}$  (see below).)

As for V19E, the P47S mutation occurs in a single turn of helix linking the two clusters. The main chain conformation is somewhat different in native FdI *versus* PaFd (Fig. 8B), with a difference in the C $\alpha$  positions at the site of mutation of ~1.6 Å. Consequently, the C $\alpha$ –C $\beta$  orientation of Ser<sup>47</sup> in P47S FdI is different from that of Ser<sup>44</sup> in PaFd, but due to the conformation of the Ser<sup>47</sup> side chain, the O $\gamma$  atoms of the two Ser are fairly close in space, 1.43 Å apart in the superposition. The closest distance to the  $[\text{4Fe-4S}]^{2+/1+}$  clusters also remains about

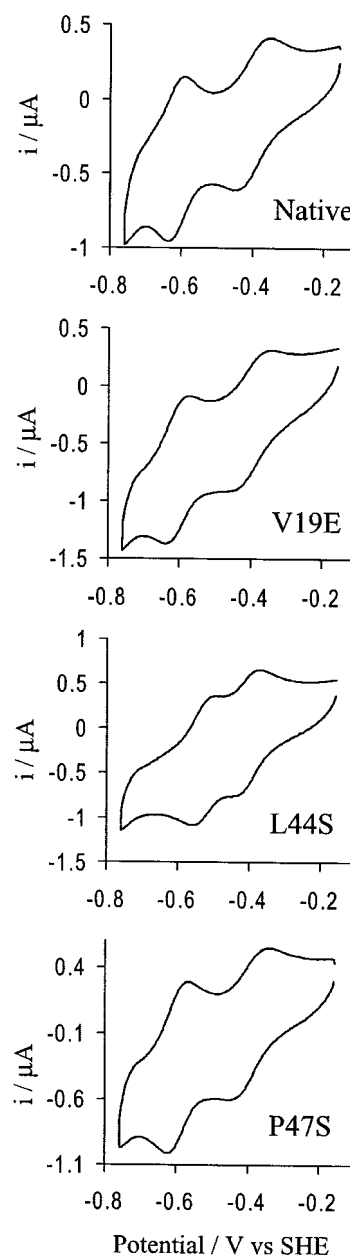


FIG. 6. Bulk solution cyclic voltammetry of native and FdI variants at 0 °C, pH 7.0. Conditions were as follows: 60 mM mixed buffer, 0.1 M NaCl, and 4 mM neomycin at 0 °C, pH 7.0. Scan rate was 5 mV s<sup>-1</sup>. Protein concentrations were in the range of 0.05–0.1 mM. Voltammograms were measured on the third cycle.

TABLE I  
Observed  $E^{0'}$  for FdI variants

$E^{0'}$  in mV *versus* standard hydrogen electrode is shown. Experimental values were obtained at 0 °C and pH 7.0 in the presence of 4 mM neomycin.

FdI variant	$E^{0'}$ $[\text{4Fe-4S}]^{2+/1+}$ mV	Observed $\Delta E^{0'}$
Native	-619	Reference
V19E	-606	+13
L44S	-525	+94
P47S	-596	+23

the same at 9.3–10 Å. Thus, like V19E, the P47S mutation makes AvFdI more like PaFd without significant structural perturbation. Because each mutant mimics PaFd better, this is consistent with the slightly higher  $E^{0'}$  in both cases.

**L44S**—The L44S variant gave a large increase in  $E^{0'}$  of 94

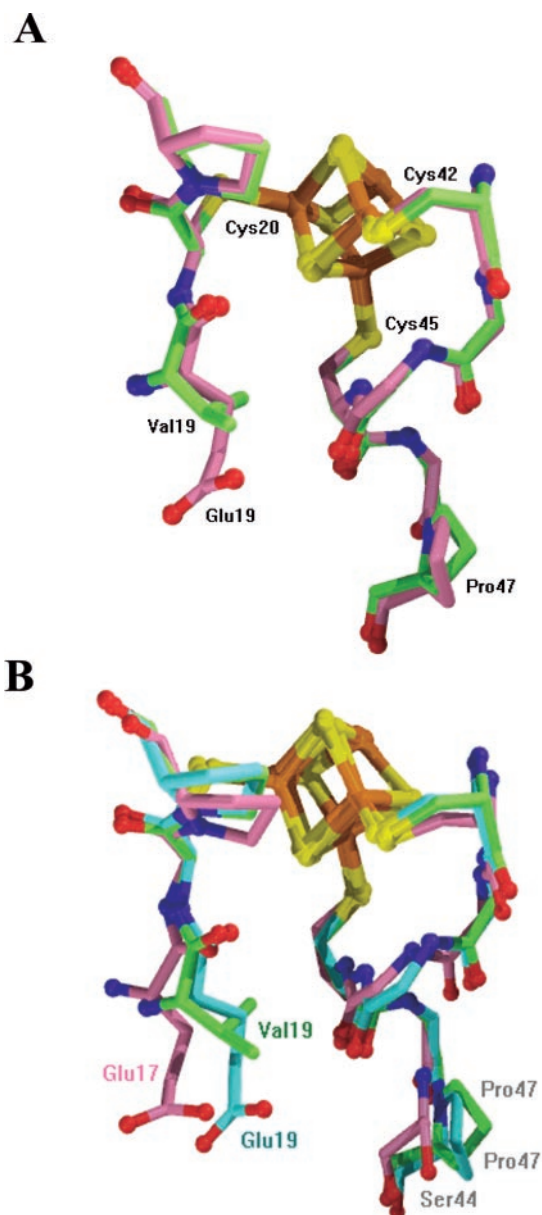


FIG. 7. Details of the V19E AvFdl mutant structure and comparison with native AvFdl and PaFdl. *A*, superposition of residues 19–21 and 42–47 of native AvFdl (green) and mutant AvFdl (pink) with the corresponding [4Fe-4S] clusters. The root mean square deviation between native and V19E AvFdl is 0.229 Å following least squares fit of all 526 main chain and C $\beta$  atoms. *B*, superposition of residues 19–21 and 42–47 of native AvFdl (green) and mutant AvFdl (blue), residues 17–19 and 39–44 of PaFdl (pink), and the corresponding [4Fe-4S] clusters. The V19E mutation makes AvFdl like PaFdl at this position. PaFdl and native AvFdl are superposed as in Fig. 2*B*, and the views are similar to that shown in Fig. 2*B*.

mV, consistent with the proposal that this position is a critical determinant for  $E^0$  (46). Its structure was refined to 2.2-Å resolution and revealed that there were four copies in the asymmetric unit in two “dimers” in the C2 space group. The density for the four copies at Ser<sup>44</sup> varies from very strong to weak, but all four are modeled with confidence. Fig. 9*A* compares the four copies with each other, and Fig. 9*B* compares copy A to native Fdl in the vicinity of the [4Fe-4S]<sup>2+/+</sup> cluster. The four independent copies of L44S are very similar, with root mean square deviations of 0.24–0.39 Å overall. However, there is some variation at the site of the mutation, apparently accounting for the four copies in the crystallographic asymmetric

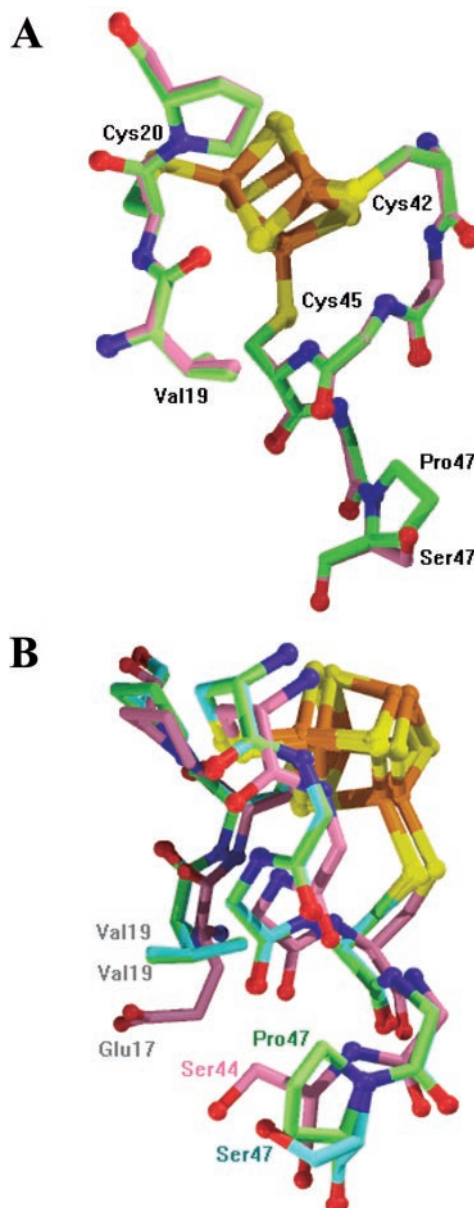
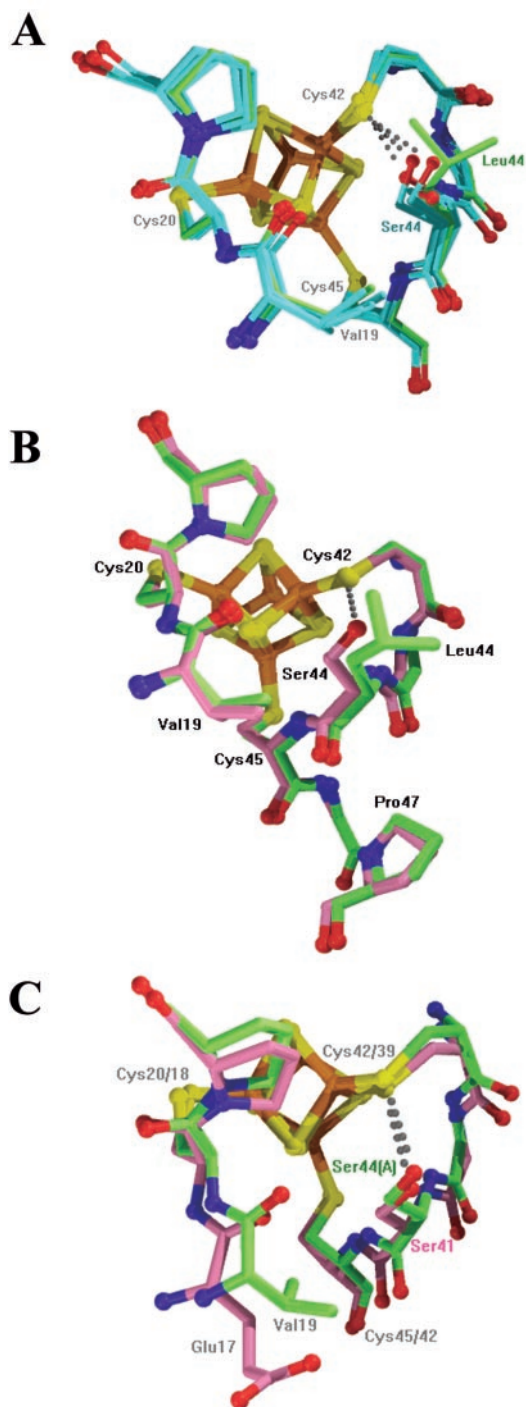


FIG. 8. Details of the P47S AvFdl mutant structure and comparison with native AvFdl and PaFdl. *A*, superposition of residues 19–21 and 42–47 of native AvFdl (green) and mutant AvFdl (pink) with the corresponding [4Fe-4S] clusters. The root mean square deviation between native and P47S AvFdl is 0.108 Å following least squares fit of all 526 main chain and C $\alpha$  atoms. *B*, superposition of residues 19–21 and 42–47 of native AvFdl (green) and mutant AvFdl (blue), residues 17–19 and 39–44 of PaFdl (pink), and the corresponding [4Fe-4S] clusters. The P47S mutation makes AvFdl like PaFdl at this position. PaFdl and native AvFdl are superposed as in Fig. 2*B*, and the views are similar to that shown in Fig. 2*B*.

unit. This suggests that the Leu-to-Ser substitution in the context of the AvFdl sequence (Cys-Ala-Leu/Ser-Cys) versus the PaFdl (Cys-Gly-Ser-Cys) sequence is not energetically favorable, giving rise to the alternate conformations. A similar effect was observed for an earlier I40N replacement (32). Consequently, the C $\alpha$  positions of Ser<sup>44</sup> vary by up to 0.8 Å from each other. The *B* values of Ser<sup>44</sup> in the four copies are comparable (43–53 Å<sup>2</sup>), suggesting that all four conformations are essentially equally favorable. Perhaps a Gly at the preceding position is required for optimal stereochemistry in the constrained CXXCXXC motif.

Three of the four introduced Ser side chains are oriented such that favorable O $\gamma$ -S $\gamma$  (Cys<sup>42</sup>) hydrogen bonds can be



**FIG. 9. Details of the L44S AvFdl mutant structures and comparison to native AvFdl and PaFd.** *A*, superposition of residues 19–21 and 42–47 of native AvFdl (green) and four independent copies of the L44S mutant of AvFdl (blue) with the corresponding [4Fe-4S] clusters. In copies A, B, and D of L44S AvFdl, the side chain of Ser<sup>44</sup> is oriented such that a hydrogen bond from O<sub>γ</sub> to S<sub>γ</sub> of Cys<sup>42</sup> can be formed (3.39, 3.42, and 3.67 Å, respectively), indicated by gray dotted lines. The root mean square deviations between native AvFdl and four copies of the L44S mutant are 0.276, 0.337, 0.321, and 0.256 Å for the A, B, C, and D copies, respectively, following least squares fit of all 526 main chain and C<sub>β</sub> atoms. *B*, superposition of residues 19–21 and 42–45 of native AvFdl (green) and copy A of the L44S mutant of AvFdl (pink) with the corresponding [4Fe-4S] clusters. *C*, superposition of residues 19–21 and 42–45 of copy A of L44S AvFdl (green) with residues 17–19 and 39–42 of PaFd (pink) based on their common superposition onto native AvFdl as in Figs. 2B, 9A, and 9B. Both structures exhibit a hydrogen bond between Ser<sup>44</sup>/Ser<sup>41</sup> and the corresponding [4Fe-4S] cluster ligands Cys<sup>42</sup>/Cys<sup>39</sup> (3.39/3.45 Å), shown by gray dotted lines as in Figs. 2B, 9A, and 9B.

formed. For copies A, B, and D, the geometry and contacts are consistent with a hydrogen bond of 3.4–3.6 Å from the serine hydroxyl to S<sub>γ</sub> of Cys<sup>42</sup>. The conformation of these side chains is very similar to the corresponding Ser in PaFd as illustrated in Fig. 9C, which compares the structure of that protein to copy A of L44S Fd. As shown, the same hydrogen bond occurs in PaFd (new Protein Data Bank file 1DUR). Although the contact between the O<sub>γ</sub> of Ser<sup>44</sup> and the S<sub>γ</sub> of Cys<sup>42</sup> is roughly orthogonal to the C<sub>β</sub>–O<sub>γ</sub> and C<sub>β</sub>–S<sub>γ</sub> bonds, the hydrogen atom on O<sub>γ</sub> can point almost directly at the S<sub>γ</sub>, because unlike a main chain amide, it is bonded to the O<sub>γ</sub> at 109° (sp<sup>3</sup> bond). The introduction of this dipole in at least three-fourths of the copies (if the crystal conformations are averaged in solution) is clearly the primary factor in the elevated  $E^{0'}$  of PaFd versus native AvFdl or L44S versus native Fdl.

In addition to the introduction of an OH–S bond, the presence of the Ser side chain results in ordered water molecules involved in hydrogen bonds with Ser<sup>44</sup> and adjacent residues (3, 1, 0, and 2 additional water molecules in copies A, B, C, and D, respectively, compared with native Fdl). While not in direct contact with the atoms of the [4Fe-4S]<sup>2+/+</sup> cluster, the dipole moments of these ordered water molecules near the cluster could also serve to elevate  $E^{0'}$ . In particular, in copies A, B, and D, a water molecule bridges between Ser<sup>44</sup> O<sub>γ</sub> and the carbonyl of Val<sup>19</sup> and is 4.2–5.6 Å from the S<sub>γ</sub> of Cys<sup>42</sup>, the closest atom. Therefore, the presence of a Ser at position 44 not only provides a direct hydrogen bond dipole to the cluster but also provides secondary dipoles due to additional ordered water molecules at the protein surface. A water molecule at the homologous position, bridging Ser<sup>42</sup> to the carbonyl of Glu<sup>17</sup>, is also observed in PaFd, in this case 5.8 Å from S<sub>γ</sub> of Cys<sup>39</sup>, whereas no water is observed proximal to Leu<sup>44</sup> in native AvFdl, consistent with the hypothesis.

It should be noted that all of the proteins compared here have an NH–S<sub>γ</sub> hydrogen bond from residue 44 (AvFdl)/41 (PaFd)/13 (CvFd) to Cys<sup>42</sup>/Cys<sup>39</sup>/Cys<sup>11</sup>; the average distance in the four copies of L44S (3.45 Å) is comparable with that in native Fdl and PaFd (3.5 Å) and similar to CvFd (3.8 Å), so this and other features of the hydrogen bonding around the [4Fe-4S]<sup>2+/+</sup> cluster are not perturbed in the mutant and cannot be responsible for the increase in  $E^{0'}$ .

A recent study of CvFd suggested that the presence of a bulky residue at a position corresponding to position 44 of native Fdl is primarily responsible for the very low reduction potential of the [4Fe-4S]<sup>2+/+</sup> clusters found in CvFd, AvFdlIII, and AvFdl (46). The data presented here suggest instead that in the case of PaFd an ~100 mV increase in [4Fe-4S]<sup>2+/+</sup>  $E^{0'}$  relative to the corresponding cluster in AvFdl is a direct result of the presence of the OH–S bond from the serine hydroxyl to the Cys<sup>42</sup> ligand, with the positive (hydrogen) end of the introduced CH<sub>2</sub>OH side chain closest to the negatively charged S<sub>γ</sub> of the Cys<sup>42</sup> ligand, leading to an increase in  $E^{0'}$ . A secondary effect may also involve the presence of newly bound water molecules at longer distances.

**Conclusions**—The  $E^{0'}$  of the [4Fe-4S]<sup>2+/+</sup> cluster of AvFdl is ~200 mV more negative than that of the homologous cluster in PaFd. Previous mutagenesis experiments tested the contribution that individual amino acid residues make to the control of  $E^{0'}$  by converting residues in AvFdl into the corresponding residue in PaFd. Four mutations involved substitution of negatively charged surface residues with neutral residues, and two involved substitution of hydrophobic residues, but none resulted in any increase in the [4Fe-4S]<sup>2+/+</sup> cluster  $E^{0'}$ . Recently, another class of ferredoxins, represented by AvFdlIII and CvFd, was shown to contain [4Fe-4S]<sup>2+/+</sup> clusters with  $E^{0'}$  values similar to that of AvFdl (45, 46). The observation that the

sequences (Fig. 1) and structures (Fig. 2A) surrounding the very low  $E^{0'}$   $[4\text{Fe-4S}]^{2+/+}$  clusters in the dissimilar AvFdI and AvFdIII/CvFd are extremely similar encouraged the construction of three additional mutations. In this case, all three mutations led to positive increases in  $E^{0'}$ . Although Val at a position corresponding to FdI residue 19 is conserved in the low  $E^{0'}$  classes of ferredoxins, and Glu is highly conserved at the corresponding position in the higher  $E^{0'}$  ferredoxins, the minor change in  $E^{0'}$  for V19E shows that this residue is not a critical determinant of  $E^{0'}$ . A still small, but somewhat larger, change in  $E^{0'}$  of +23 mV was obtained for P47S by mimicking PaFd without modification of the FdI structure except at that position, possibly due to the introduction of the serine dipole and associated water molecules at long distances from the cluster. The largest change was observed for L44S for which an increase of 94 mV was obtained; here the environment of PaFd was reproduced by introducing an OH-S hydrogen bond from the serine hydroxyl to the cluster ligand Cys<sup>42</sup> with accompanying movement of water. Since the residue at position 44 is not conserved in either the high or the low  $E^{0'}$  classes of  $[4\text{Fe-4S}]^{2+/+}$  clusters, future experiments will be aimed at determining the influence that other residues at this position have on reduction potential.

## REFERENCES

- Beinert, H., Holm, R. H., and Münck, E. (1997) *Science* **277**, 653–659
- Holm, R. H., Kennepohl, P., and Solomon, E. I. (1996) *Chem. Rev.* **96**, 2239–2314
- Johnson, M. K. (1994) in *Encyclopedia of Inorganic Chemistry* (King, R. B., ed) Vol. 4, pp. 1896–1915, John Wiley & Sons, Inc., New York
- Beinert, H. (2000) *J. Biol. Inorg. Chem.* **5**, 2–15
- Stout, C. D. (2001) in *Handbook of Metalloproteins* (Messerschmidt, A., Huber, R., Poulos, T., and Wieghardt, K., eds) Vol. I, pp. 560–573, John Wiley & Sons, Chichester, UK
- Sieker, L. C., and Adman, E. T. (2001) in *Handbook of Metalloproteins* (Messerschmidt, A., Huber, R., Poulos, T., and Wieghardt, K., eds) Vol. I, pp. 574–592, John Wiley & Sons, Chichester, UK
- Bertini, I., Gori-Savellini, G., and Luchinat, C. (1997) *J. Biol. Inorg. Chem.* **2**, 114–118
- Przysiecki, C. T., Meyer, T. E., and Cusanovich, M. A. (1985) *Biochemistry* **24**, 2542–2549
- Luchinat, C., Capozzi, F., Borsari, M., Battistuzzi, G., and Sola, M. (1994) *Biochem. Biophys. Res. Commun.* **203**, 436–442
- Stephens, P. J., Jollie, D. R., and Warshel, A. (1996) *Chem. Rev.* **96**, 2491–2513
- Heering, H. A., Bultink, Y. B. M., Hagen, W. R., and Meyer, T. E. (1995) *Eur. J. Biochem.* **232**, 811–817
- Iwagami, S. G., Creach, A. L., Haynes, C. A., Borsari, M., Felli, I. C., Piccioli, M., and Eltis, L. D. (1995) *Protein Sci.* **4**, 2562–2572
- Soriano, A., Li, D., Bian, S., Agarwal, A., and Cowan, J. A. (1996) *Biochemistry* **35**, 12479–12486
- Bian, S., Hemann, C. F., Hille, R., and Cowan, J. A. (1996) *Biochemistry* **35**, 14544–14552
- Sola, M., Cowan, J. A., and Gray, H. B. (1989) *Biochemistry* **28**, 5261–5268
- Bertini, I., Luchinat, C., and Rosato, A. (1996) *Prog. Biophys. Mol. Biol.* **66**, 43–80
- Denke, E., Merbitz-Zahradnik, T., Hatzfeld, O. M., Snyder, C. H., Link T. A., and Trumppower, B. L. (1998) *J. Biol. Chem.* **271**, 9085–9093
- Schroter, T., Hatzfeld, O. M., Gemeinhardt, S., Korn, M., Friedrich, T., Ludwig, B., and Link T. A. (1998) *Eur. J. Biochem.* **255**, 100–106
- Eidsness, M. K., Burden, A. E., Richie, K. A., Kurtz, D. M., Jr., Scott, R. A., Smith, E. T., Ichiye, T., Beard, B., Min, T., and Kang, C. (1999) *Biochemistry* **38**, 14803–14809
- Carter, C. W., Jr. (2001) in *Handbook of Metalloproteins* (Messerschmidt, A., Huber, R., Poulos, T., and Wieghardt, K., eds) Vol. I, pp. 602–609, John Wiley & Sons, Chichester, UK
- Macedo, A. L., Besson, S., Moreno, C., Fauque, G., Moura, J. J., and Moura, I. (1996) *Biochem. Biophys. Res. Commun.* **229**, 524–530
- Backes, G., Mino, Y., Loehr, T. M., Meyer, T. E., Cusanovich, M. A., Sweeney, W. V., Adman, E. T., and Sanders-Loehr, J. (1991) *J. Am. Chem. Soc.* **113**, 2055–2064
- Rees, D. C. (1985) *Proc. Natl. Acad. Sci. U. S. A.* **82**, 3082–3085
- Mauk, A. G., and Moore, G. R. (1997) *J. Biol. Inorg. Chem.* **2**, 119–125
- Náray-Szabó, G. (1997) *J. Biol. Inorg. Chem.* **2**, 135–138
- Warshel, A., Papazyan, A., and Muegge, I. (1997) *J. Biol. Inorg. Chem.* **2**, 143–152
- Moore, G. R. (1983) *FEBS Lett.* **161**, 171–175
- Schejter, A., and Eaton, W. A. (1984) *Biochemistry* **23**, 1081–1084
- Shen, B., Jollie, D. R., Stout, C. D., Diller, T. C., Armstrong, F. A., Gorst, C. M., La Mar, G. N., Stephens, P. J., and Burgess, B. K. (1994) *J. Biol. Chem.* **269**, 8564–8575
- Jensen, G. M., Warshel, A., and Stephens, P. J. (1994) *Biochemistry* **33**, 10911–10924
- Langen, R., Jensen, G. M., Jacob, U., Stephens, P. J., and Warshel, A. (1992) *J. Biol. Chem.* **267**, 25625–25627
- Chen, K., Tilley, G. J., Sridhar, V., Prasad, G. S., Stout, C. D., Armstrong, F. A., and Burgess, B. K. (1999) *J. Biol. Chem.* **274**, 36479–36487
- Li, J., Nelson, M. R., Peng, C. Y., Bashford, D., and Noodleman, L. (1998) *J. Phys. Chem.* **102**, 6311–6324
- Meyer, J., and Moulis, J. M. (2001) in *Handbook of Metalloproteins* (Messerschmidt, A., Huber, R., Poulos, T., and Wieghardt, K., eds) Vol. I, pp. 505–517, John Wiley & Sons, Chichester, UK
- Xiao, Z., Maher, M. J., Cross, M., Bond, C. S., Guss, J. M., and Wedd, A. G. (2000) *J. Biol. Inorg. Chem.* **5**, 75–84
- Iismaa, S. E., Vázquez, A. E., Jensen, G. M., Stephens, P. J., Butt, J. N., Armstrong, F. A., and Burgess, B. K. (1991) *J. Biol. Chem.* **266**, 21563–21571
- Stombaugh, N. A., Sundquist, J. E., Burris, R. H., and Orme-Johnson, W. H. (1976) *Biochemistry* **15**, 2633–2641
- Dauter, Z., Wilson, K. S., Sieker, L. C., Meyer, J., and Moulis, J. M. (1997) *Biochemistry* **36**, 16065–16073
- Vazquez, A., Shen, B., Negaard, K., Iismaa, S., and Burgess, B. K. (1994) *Protein Exp. Purif.* **5**, 96–102
- Armstrong, F. A., Butt, J. N., and Sucheta, A. (1993) *Methods Enzymol.* **227**, 479–500
- Bard, A. J., and Faulkner, L. R. (1980) in *Electrochemical Methods: Fundamentals and Applications*, John Wiley & Sons, Inc., New York
- Matsubara, H., and Saeki, K. (1992) *Adv. Inorg. Chem.* **38**, 223–280
- Edman, E. T., Sieker, L. C., and Jensen, L. H. (1976) *J. Biol. Chem.* **251**, 3801–3806
- Moulis, J. M., Sieker, L. C., Wilson, K. S., and Dauter, Z. (1996) *Protein Sci.* **5**, 1765–1775
- Gao-Sheridan, H. S., Pershad, H. R., Armstrong, F. A., and Burgess, B. K. (1998) *J. Biol. Chem.* **273**, 5514–5519
- Kyritsis, P., Hatzfeld, O. M., Link, T. A., and Moulis, J. M. (1998) *J. Biol. Chem.* **273**, 15404–15411
- Kummerle, R., Gaillard, J., Kyritsis, P., and Moulis, J. M. (2001) *J. Biol. Inorg. Chem.* **6**, 446–451
- Fukuyama, K. (2001) in *Handbook of Metalloproteins* (Messerschmidt, A., Huber, R., Poulos, T., and Wieghardt, K., eds) Vol. I, pp. 543–552, John Wiley & Sons, Chichester, UK
- Shen, B., Jollie, D. R., Diller, T. C., Stout, C. D., Stephens, P. J., and Burgess, B. K. (1995) *Proc. Natl. Acad. Sci. U. S. A.* **92**, 10064–10068
- Shen, B., Martin, L. L., Butt, J. N., Armstrong, F. A., Stout, C. D., Jensen, G. M., Stephens, P. J., La Mar, G. N., Gorst, C. M., and Burgess, B. K. (1993) *J. Biol. Chem.* **268**, 25928–25939
- Martin, A. E., Burgess, B. K., Stout, C. D., Cash, V. L., Dean, D. R., Jensen, G. M., and Stephens, P. J. (1990) *Proc. Natl. Acad. Sci. U. S. A.* **87**, 598–602